Production of polyurethane/nano-hydroxyapatite hybrid materials and microstructural characterization

A.B. Martínez-Valencia, G. Carbajal-De la Torre, E. Torres-Sanchez, L. Tellez-Jurado and H.E. Esparza-Ponce.

Abstract

In the present work, the polyurethane/nanohydroxyapatite hybrid materials were prepared with different content of nHA (0, 10, 20, 30, and 40% weight) as filler. The nanohydroxyapatite powders were synthesized by hydrothermal synthesis and by ultrasound-assisted co-precipitation methods. The synthesis of polyurethane was carried out by a two-step polymerization method using 1,6-diisocyanate hexane, polycaprolactone and 1,4-butanediol as precursors. The nHA was added in situ during the polymerization reaction. The structure, microstructure, specific surface and thermal stability were determinate by XRD, FTIR, SEM, DTA-TGA, DSC and water absorption measurements. The results show that the synthesized nanohydroxyapatite powders were composed of micrometric and mesoporous aggregates of nanocrystalline hydroxyapatite particles (Dc ≤ 40 nm), in addition, since nanohydroxyapatite powders are prepared via ultrasound-assisted co-precipitation showed high surface area values (97.9 m^2g^{-1}) and homogeneous chemical composition, these ones were used for the fabrication of hybrid materials which were successfully prepared by the incorporation in situ of nanohydroxyapatite during the polymerization process. The obtained materials showed different behavior during water absorption tests as well as thermal stability as a function of filler content.

Keywords: Polyurethane, nanohydroxyapatite, hydrothermal synthesis, ultrasound-assisted co-precipitation.

Introduction

Nowadays, bone regeneration is one of the most intensively studied topics in the tissue engineering research field. In the past decade important advances on the design and fabrication of bone graft substitutes have been reached (Boccaccini and Gough, 2007; Guelcher 2008; Gorna and Gogolewski, 2003; Kalita et al., 2007; Suchanek and Yoshimura, 1998; Wang 2003; Dong et al., 2008, 2009).

Just like other biomaterials, bone graft substitutes have to comply not only with certain mechanical behavior but also to comply with the properties of biocompatibility in order to guarantee their correct interaction with the human body (Griesser 1991; Nair and Laurencin, 2007; Park and Bronzino, 2003; Vermette et al., 2001; Ramakrishna et al., 2001).

The different tested biomaterials as potential bone grafts which include: ceramics, polymers, metals, composites and hybrid materials. The hybrid materials based on polymeric matrix with an inorganic nanostructured filler have shown excellent properties, which are attributed as a result not only to the characteristics inherent to each phase in the hybrid, but also to the interaction between them; that is, the characteristics of matrix-filler bond and interface (Ramakrishna et al., 2001; Zhao et al., 2008; Zhi-hua et al., 2007), for example, the polyurethane/hydroxyapatite hybrids (PU/HA), which combine intrinsic physicochemical characteristics of the polymer matrix such as biocompatibility with the well know bioactive properties of the HA filler that promotes the osteogenesis (Zhao and Zhang, 2008). In addition, it is believed that the

incorporation of the HA phase into the polymeric matrix promotes the water absorption through the interface generated between the polymer and the more hydrophilic bioactive phases, which modifies the degradation kinetic of the material (Santosa et al., 2002). In the present work, the fabrication of a series of polyurethane/nano-hydroxyapatite (PU/nHA) hybrids is reported, giving special emphasis to the effect of both, the filler characteristics and content as well as the synthesis pathway on the microstructural characteristics of the obtained hybrid materials.

Materials and methods

Materials synthesis

nHA synthesis: The starting nHA powders were synthesized through the wet chemical methods of hydrothermal and ultrasound-assisted coprecipitation.

For hydrothermal route (nHA1), powders were prepared by mixing stoichiometric quantities (Ca/P = 1.67) of calcium nitrate tetrahydrate $Ca(NO_3)_2 \cdot 4H_2O$ and diammonium hydrogen phosphate $(NH_4)_2HPO_4$ precursor solutions. Before mixing, the pH value of the solutions was adjusted above 10 with ammonium hydroxyl solution (NH_4OH). The hydrothermal synthesis was carried out under autogenous pressure employing a Teflon-lined stainless steel autoclave which was heating at 175°C for 15 h.

In the case of ultrasound-assisted co-precipitation route (nHA2), powders have been prepared by mixing the stoichometric quantities (ratio Ca/P = 1.67) of both $Ca(NO_3).4H_2O$ and $(NH_4)_2HPO_4$ solutions. The pH value of mixed solution was adjusted to 8.5 to 9 using NH4OH. The reaction was carried out under ultrasonic treatment using an ultrasonic bath at 80±2°C for 30 min. In order to obtain a well crystallized product, once the precipitation process was concluded, the sonochemical process was keep by

30 min further (Gedanken, 2004). In both cases, the obtained powders were washed with distilled water several times and subsequently dried at 85°C for 24 h.

PU/nHA hybdrids synthesis: Hybrid materials were synthesized via two-step polymerization method (Rogers and Long, 2003), using 1,6-diisocyanato hexane (HDI), polycaprolactone (PCL) with molecular weight of 80,000, 1,4-butanediol (BD) as starting materials and N,Ndimethylformamide (DMF) and dibutyltin diacetate (DBTDA) as solvent and catalyst, respectively.

Polymerization reaction was carried out in a three-necked round bottom flask under an inert atmosphere, the reaction system was equipped with a water cooling condenser, mechanical stirrer and a thermometer. The stoichiometry of the reaction was 3: 2: 1 of HDI: PCL: BD respectively.

First, PCL pellets were dried between 70 to 80°C under vacuum for 1 h in order to remove the residual water. Later, once PCL pellets were dried and the system was degassed, nHA (0, 10, 20, 30, 40% weight) powders were added into the bottom flask, the reagents were mixed with 20 ml DMF and DBTDA. The reaction was conducted at 80°C adding dropwise HDI under mechanical stirring of 400 rpm for 2 h.

In the second step, the prepolymer solution was extended by the addition of BD, and the reaction was continued at 80°C for 2 h more. The polymer solution containing nHA powders was precipitated in distilled water and finally the hybrids were dried at 50°C for 24 h.

Materials characterization: The microstructural analyses of the samples were carried out by several techniques. The crystalline state and the identification of phases were verified by X-ray diffraction (XRD) analysis and performed with a diffractometer

model Bruker D8 Advance. Diffraction patterns were acquired ranging from 10 to 70° in 2θ at a scanning speed of 0.2°/min using the $K\alpha_{Cu}$.

Fourier-transformed infrared spectroscopy (FT-IR) was used to identify the characteristic functional groups corresponding to the nHA and PU as well as the possible bonding between PU and nHA. Powder samples (0.003 g) were carefully mixed with 0.3 g of KBr (infrared grade) and pelletized under pressure of 2 tons for 1 min. The samples were analyzed using a Bruker-Tensor 27 spectrophotometer in the range of 4000 to 400 cm^{-1} at 1 cm^{-1} of resolution.

N_2 physisorption isotherms were measured using a BEL apparatus. Specific surface area values of nHA were calculated by BET method (SBET) and pore size distribution was calculated by BJH method.

Microstructure, morphology and composition analysis of the different samples were performed by electron microscopy techniques. Scanning electron microscopy was performed using a SEM-JEOL 6400 at 15 kV. The elemental composition was realized by energy dispersive X-ray spectroscopy (EDS) and the instrument was operated at 15 kV. The hybrid specimens were cut using a diamond razor blade parallel to the surface and the samples were sputter-coated with Au prior to examination. For transmission electron microscopy (TEM) a microscope model JEOL JEM2200FS, operating at 200 kV was used.

Thermogravimetric analyses (TGA) were performed to investigate the thermal stability of the different hybrids. Samples with an average weight of 3 to 12 mg were used for the measurements. The samples were scanned at the heating rate of 5°C/min

under a constant purge flow rate of nitrogen of 100 ml/ min. The samples were scanned in the range of 30 to 600°C.

Thermal transitions of the hybrids were analyzed with a differential scanning calorimeter (DSC TA instruments 2920) from - 60 to 120°C with a heating rate of 5°C/min. The reported transitions were taken from first and second heating scans at a heating/cooling. Glass-transition temperatures (T_g) for the polymer samples were taken as an inflection point on curves of heatcapacity changes. Melting temperatures (T_m) for polymer samples were read at endothermic-peak maxima.

Analysis of water absorption was carried out according to ASTM D570. Three cylinders of the samples of each composition were tested after drying to a constant weight and their weights recorded and were immersed into a polystyrene bottle with 30 ml of distilled water at 37°C at time intervals of 1, 2, 4, 8, 12, 24, 48 and 72 h. Later at a specified time, the hybrids were removed from the water and weighed to an accuracy of ±0.0001 g on an analytical balance, after to surface water had been removed with paper. The weight change expressed in percent of each specimen due to the immersion was calculated using the expression:

$$\text{Water absorption WS (\%)} = (W_2 - W_1) / W_1 \times 100 \quad (1)$$

Where W_2 is the wet weight and W1 is the dry weight before immersion.

For practical purpose, the samples were named as follow: hybrid containing 0% weight of nHA was labeled as (PU), containing 10% weight of nHA as (HA10), and 20% weight of nHA as (HA20) and so on.

Results and discussion

Characterization of nHA powders: The use of nanometric ceramic powders have revolutionized the field of biomaterials, due better interaction contributed by large surface area and that generally shown superior biological activity and even in some cases osteoinductive properties (Kalita et al., 2007). A number of powder processing techniques have been developed and used to synthesize HA as reported in the literature including aqueous precipitation, sol–gel, solid-state, and mechano-chemical methods. In this research, firstly was investigate about an effective method to nHA with uniform nanosize, based on lowtemperature methods and ultrasonic irradiation, it is well know that ultrasonic irradiation is an effective tool to prepare nanomaterials (Gedanken, 2004). Figure 1 shows the XRD patterns of synthesized nHA powders by hydrothermal synthesis (nHA1) and ultrasound-assisted co-precipitation (nHA2). Result indicates that the obtaining phase is crystalline hydroxyapatite, which was identified by the JCPDS card 01-071-5049 as synthetic hexagonal hydroxyapatite, the patterns do not shown visible evidence of the presence of any common secondary phases.

It means that pure and homogeneous nHA materials could be produced by the two methods studied. However XRD pattern profiles indicate certain variation on crystal size of the nHA as a result of the synthesis method; specifically, the sample nHA2 shows width diffraction picks which suggests the presence of a smaller size of crystallite generated as result of the acoustic cavitation caused in the process of ultrasonic irradiation.

The crystallite size of nHA powders were determined from the peak broadening using Sherrer's equation and estimated from the XRD using the reflections (002), (300) and (222). The calculated lattice constants for the hexagonal structure of nHA were

near those previously reported (a = 9.418Å, c = 6.884Å). Therefore, the variations observed on the pattern profile (Table 1) were attributed to crystal size which was influenced by the synthesis method.

The presence of phase nHA was supporting from FTIR analysis which all bands were observed (Figure 2). To both methods, a first band is observed centered at 1033 cm^{-1} together with 1095 cm^{-1} of PO_4^{3-} groups. The bands at 962, 565 and 603 cm^{-1} correspond to *n1* and *n4* symmetric PO_4^{3-} stretching vibration of the PO_4^{3-} ion. The bands assigned to the stretching modes of hydroxyl groups (OH-) in the hydroxyapatite can be clearly observed in the spectra, and they are located at 3573, 634 and 473 cm^{-1} confirmed the presence of nHA powders (Silva et al., 2003).

The two spectra did not exhibit significant differences and they showed the absorption bands characteristic to the B-type carbonated hydroxyapatite phase, in fact the bands at 1458, 1422 and 876 cm^{-1} are attributed to CO_3^{2-} ions into the structure of HA substituting PO_4^{3-} ions (Tkalcec et al., 2001).

The absorption bands at 3428 and 1650 cm^{-1} correspond to absorbed water molecules and the band at1386 cm^{-1} was attributed to residual nitrates resulting from synthesis precursors.

Nitrogen adsorption is the mainly used technique to determine surface area and to characterize the porous texture of a material, nitrogen physisorption isotherms plots are shown in Figure 3. According to IUPAC classification (Lowell et al., 2004), type II isotherm can be distinguished on the samples nHA1 (Figure 3a) and nHA2 (Figure 3b) showing an hysteresis loop type H3, corresponding to porous materials consisting of nonrigid agglomerates of plate-like particles with slit-shaped pores and are isotherms

that do not present any limiting adsorption at high partial pressures (Leofantia et al., 1998).

In addition some textural characteristics obtained from N_2 physisorption technique for the different samples is showed in Table 1. The higher surface area value 97.9 m^2g^{-1} was observed for samples synthesized by ultrasound-assisted coprecipitation technique.Figure 4a shows the SEM micrograph of the powders obtained by ultrasonic-assisted coprecipitation, the powders consist of agglomerates composed of submicrometric particles which are homogeneous on size (1 to 2 μm) and shape; besides, the composition analysis performed by EDS revealed that the Ca/P molar ratio was about 1.67 corresponding to stoichiometric hydroxyapatite (Figure 4b).

The morphology and single particle size of the nHA2 powders are show in Figure 4c, bright field TEM image shows that the particles are in the nanometric size range. Powders are constituted of almost round shaped crystals between 20 to 40 nm of large, which were directly got from various measurements on MET micrographs. This result is in good agreement with the XRD analyses (Table 1).

Based on the previous results, nHA2 powders were choose to the subsequent fabrication of nanohybrids (PU/nHA) due that ultrasound-assisted coprecipitation method reduced significantly the time of synthesis of the nHA (1 h), provides a minor crystal size (20 to 40 nm) and high surface area values (97.9 m^2g^{-1}) implicating major interface and they are able to promote a better interaction between filler-matrix.

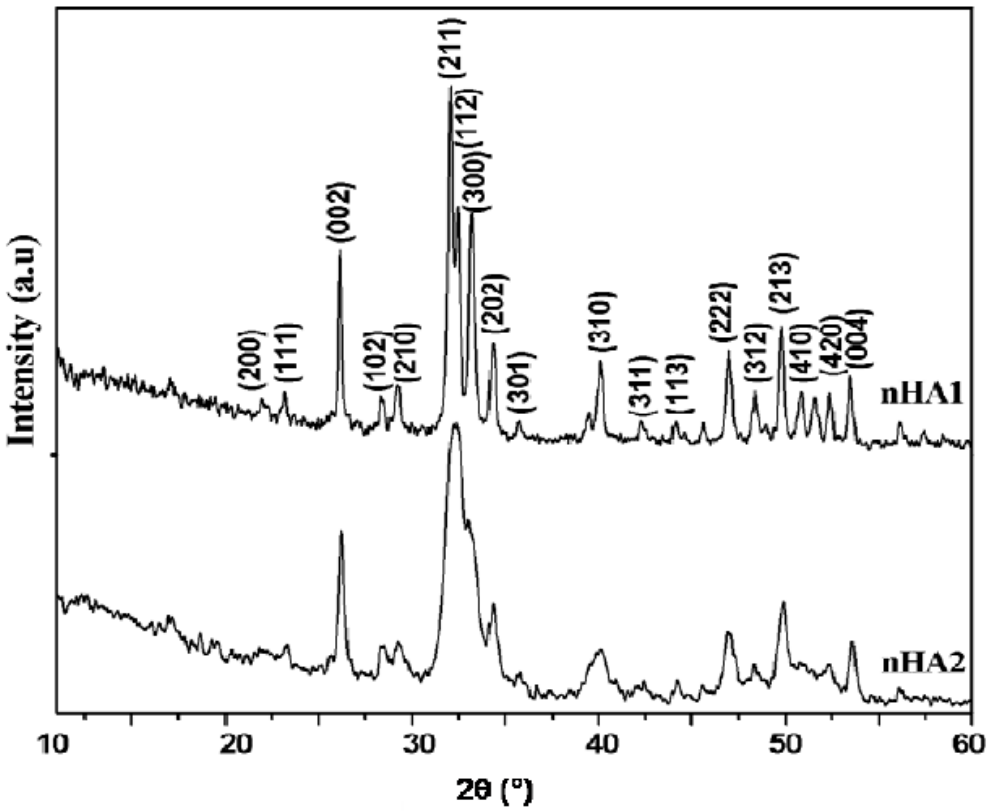

Figure 1. XRD patterns of nHA synthesized by hydrothermal synthesis (nHA1) and ultrasound-assisted co-precipitation (nHA2).

Table 1. Cell parameters and textural characteristics of nHA powder.

Sample	Cell parameter (Å)		Crystallite size (nm)			BET surface area (m^2g^{-1})	Mean pore diameter (nm)	Total pore Volume (cm^3g^{-1})
	a	c	(002)	(300)	(222)			
nHA1	9.353	6.846	38	25	19	70.30	25.8	0.464
nHA2	9.329	6.844	23	-	16	97.97	24.2	0.593

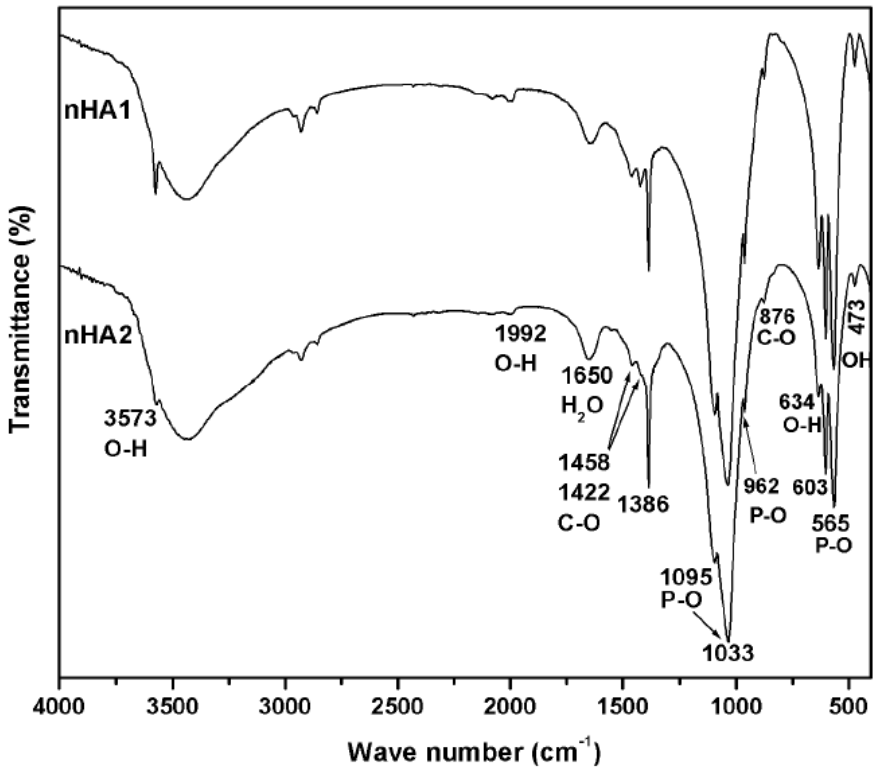

Figure 2. FTIR spectra of nHA obtained by hydrothermal synthesis (nHA1) and ultrasound-assisted co-precipitation (nHA2).

From now on nHA2 powders are named only as nHA. Figure 5 shows the XRD patterns for the series of hybrid materials containing different PU/nHA ratios. All the displayed reflexions on the PU/nHA hybrids XRD pattern were identified, then picks observed at 2θ = 26°, 32°, 32.4°, 33° corresponding to (002), (211), (300), (202) respectively and other less intense at 40° corresponding to (310) reflections identified of crystalline nHA. In addition, pick observed at 21 to 24° is related to HDI-based polyurethane phase exposing partially crystalline structures (Rogulska et al., 2006). It is noticeable that the fact that in spite of the in situ incorporation of nHA during the polymerization, the filler preserve its crystalline state.

FTIR spectra of the hybrids (Figure 6) showed the typical absorption bands of hydroxyapatite, together with a characteristic band of polyurethane. All the hybrids

showed absorption of urethane group: a large carbonyl peak is noted at 1731 cm^{-1} assigned to free hydrogenbonded C = O stretching, resulting from the ester groups of polyurethane, the carbonyl stretching region (1600 to 1840 cm^{-1}) is dominated by the intense soft segment ester band located at 1731 cm^{-1} which depending on the presence of soft segment (polycaprolactone) crystallinity.

At 1555 cm^{-1} corresponds to hydrogen-bonded –NH groups and absorption at 3440 cm^{-1} to nonbonded –NH groups (Skarja and Woodhouse, 2000). The bands at 2945 and 2868 cm^{-1} were associated with C-H asymmetric and symmetric stretching of CH_2 groups.

For the nHA, the PO_4^{3-} bands are detected at 565, 1035, 602, 964 and 1099 cm^{-1}. It is noticeable that OH^- stretching vibration at 3573 cm^{-1} is not observed of the hybrids; this fact, would suggest a bonding between PU and nHA.

Figures 7a and b shows the SEM images corresponding to the cross-section of PU and the hybrids samples, respectively. The PU (Figure 7a) possesses an interconnected irregular porous structure which can be produced by the presence of gas bubbles occluded during the processing, most of the pores were less than 10 μm in size. The blended PU/nHA possesses a combination of the individual PU and nHA morphologies (Figure 7b). The observed microstructure appears to be constituted of nHA crystals embedded (in some cases agglomerates) in the polyurethane continuous matrix. The pore size was estimated between 1 and 2 μm for PU/nHA hybrids. Therefore the manipulation of physical structures such as morphology and hybrid surface could also be modified and so improve its physiological functions (Boccaccini and Gough, 2007). EDS analysis showed that a relatively homogeneous distribution of

Ca and P elements are present in the hybrid indicated that the nHA powders were homogeneously dispersed in PU matrix and further confirms that the hybrids were successfully fabricated. Figure 8 shows the elemental analysis of mapping results of HA20 hybrid.

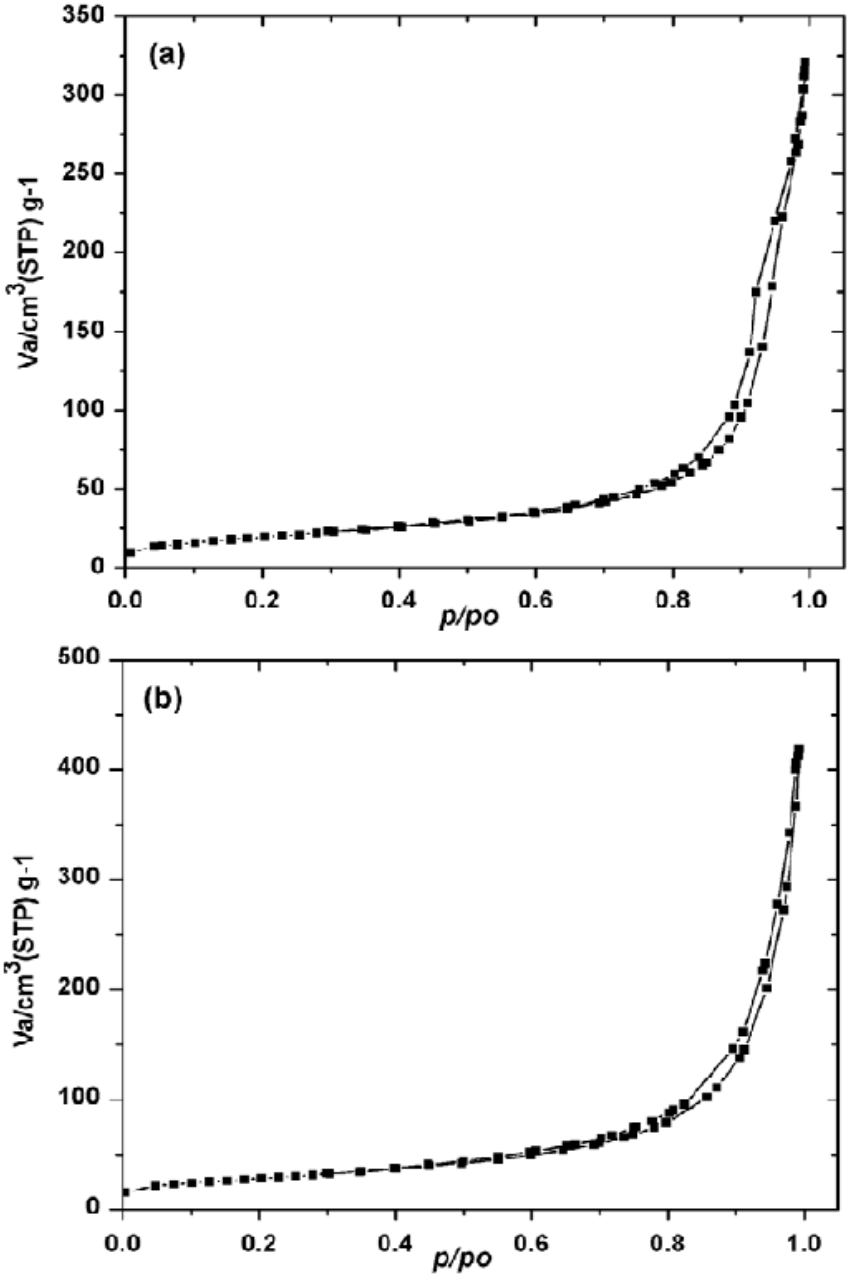

Figure 3. Hysteresis of nitrogen adsorption isotherms, (a) nHA1 and (b) nHA2.

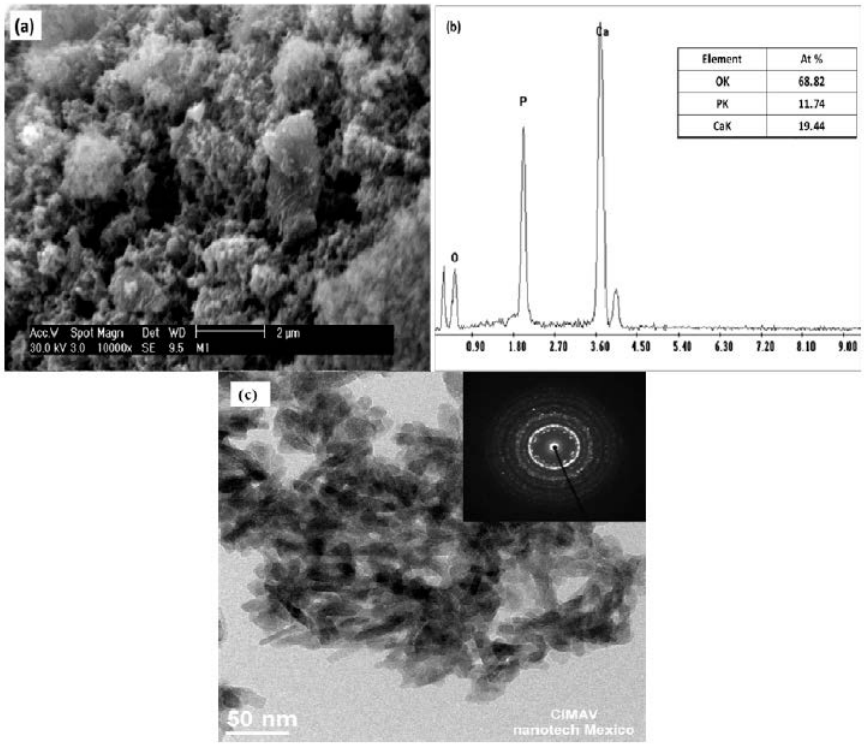

Figure 4. (a) SEM image of nHA2 aggregates, (b) EDS spectrum and (c) bright field TEM micrographs with insert of electron diffraction pattern.

Termoanalytic techniques are vitals in materials characterization to know the fabrication processes and to take a control about the material fabrication, thermal decomposition behavior of PU and hybrids was studied by thermogravimetry (TG). The thermogravimetric plot of the hybrid materials are shown in Figure 9, it is observed two thermal process, one that begins at about 200°C and is essentially complete at 330°C corresponding to the weight loss of PU and the second thermal process between 300 to 450°C associated with the removal of organic phase from the hybrids and it displays similar features for the different hybrid materials (Figure 9a). The materials with 30 and 40% of nHA were least stable, while the materials with minor contain of nHA (HA10 and HA20) were the most thermally stable compared to pure PU. The thermal stability of the nanohybrids is significantly improved as a result of incorporation nHA in PU.

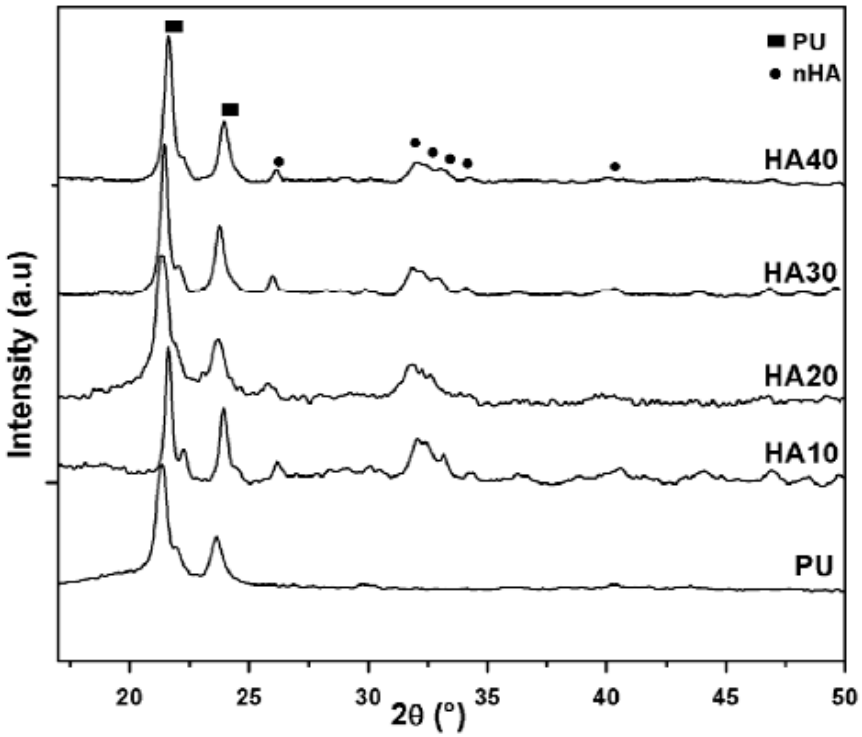

Figure 5. XRD patterns for the different hybrids.

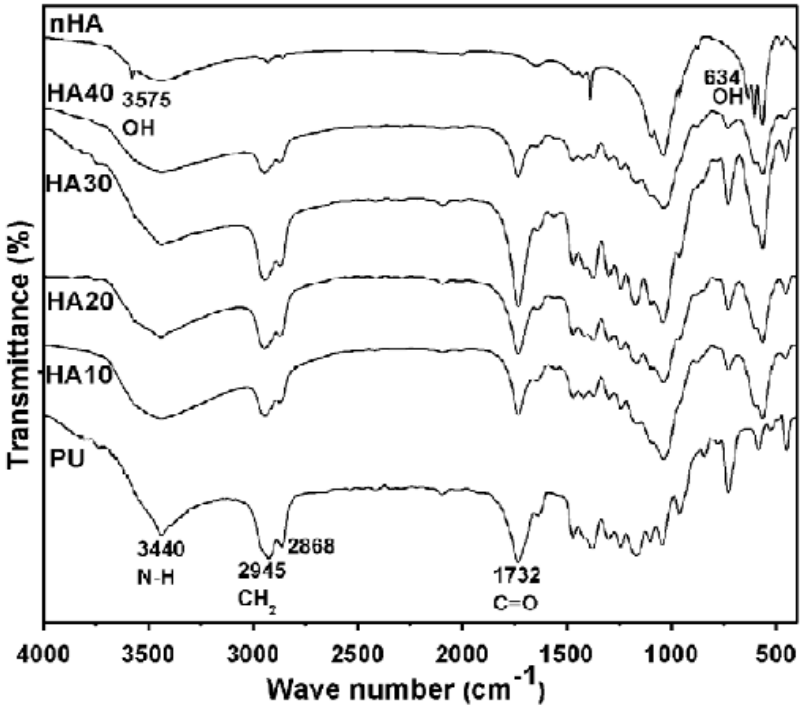

Figure 6. FT-IR spectrum of PU/nHA different hybrids.

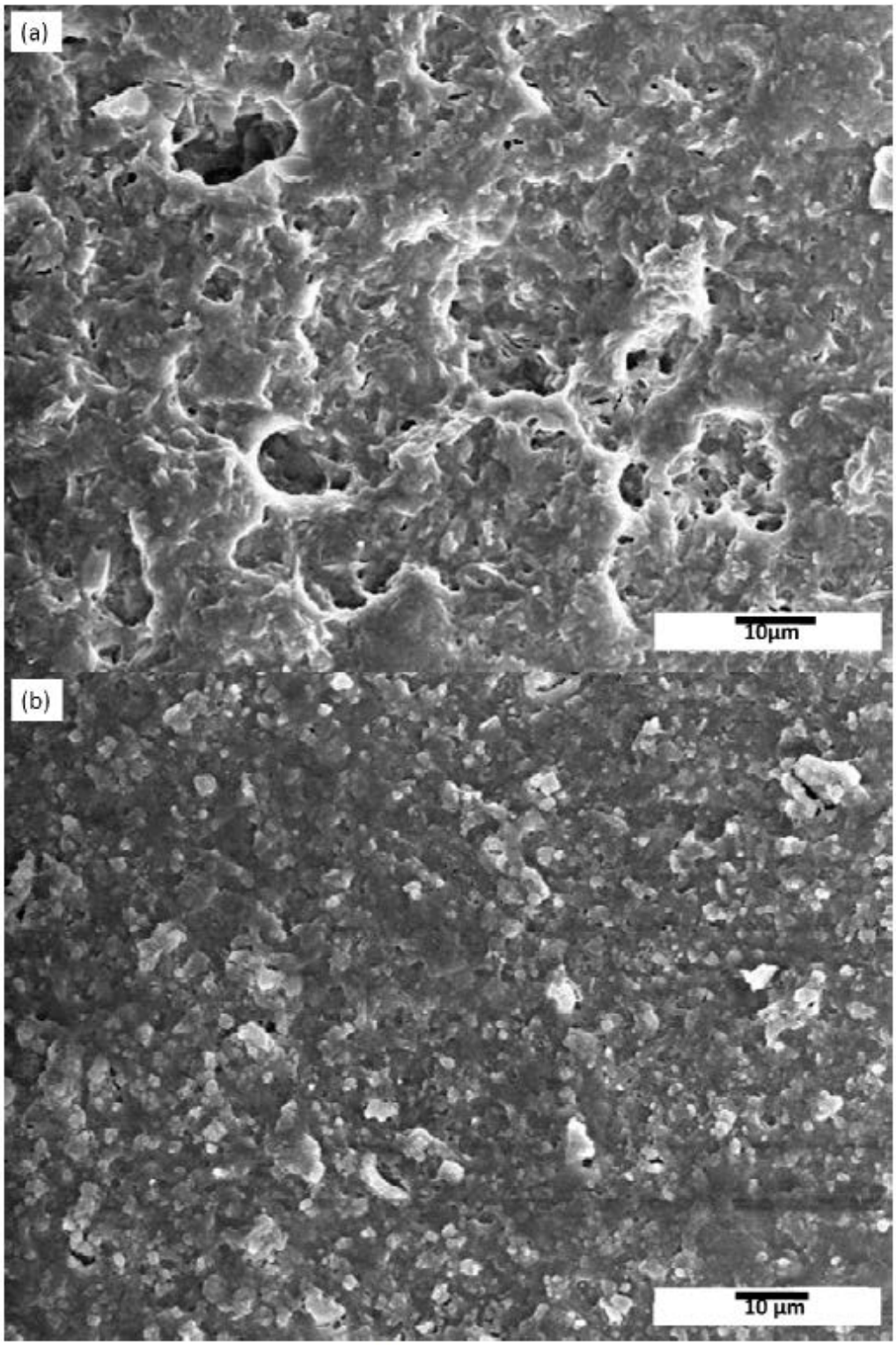

Figure 7. SEM image of sample, (a) PU and (b) HA10.

DTA curves for PU/nHA hybrids are represented in Figure 9b. The first endothermic peak observed at DTA curves at about 64 to 65°C is attributed to melting events (T_m), independent on the content of nHA. The subsequent strong endothermic peak at about 300°C for PU and 400°C for PU/nHA, results from the combustion of organic material (PU).

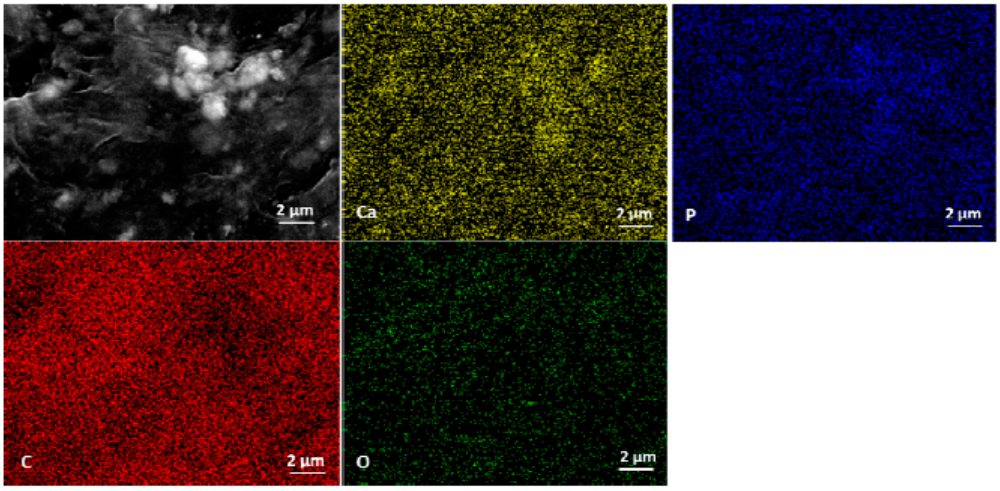

Figure 8. Electron micrograph and corresponding mapping of HA20 hybrid showing Ca, P, C and O distribution.

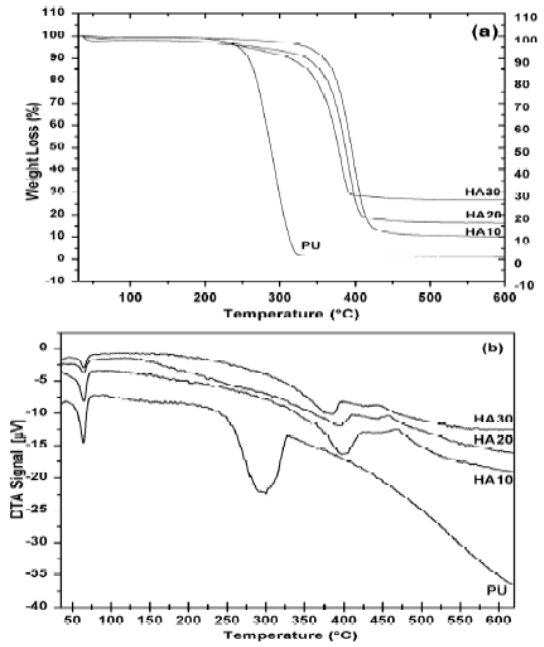

Figure 9. (a) Thermogravimetric and (b) differential thermal analysis of the PU/nHA hybrids.

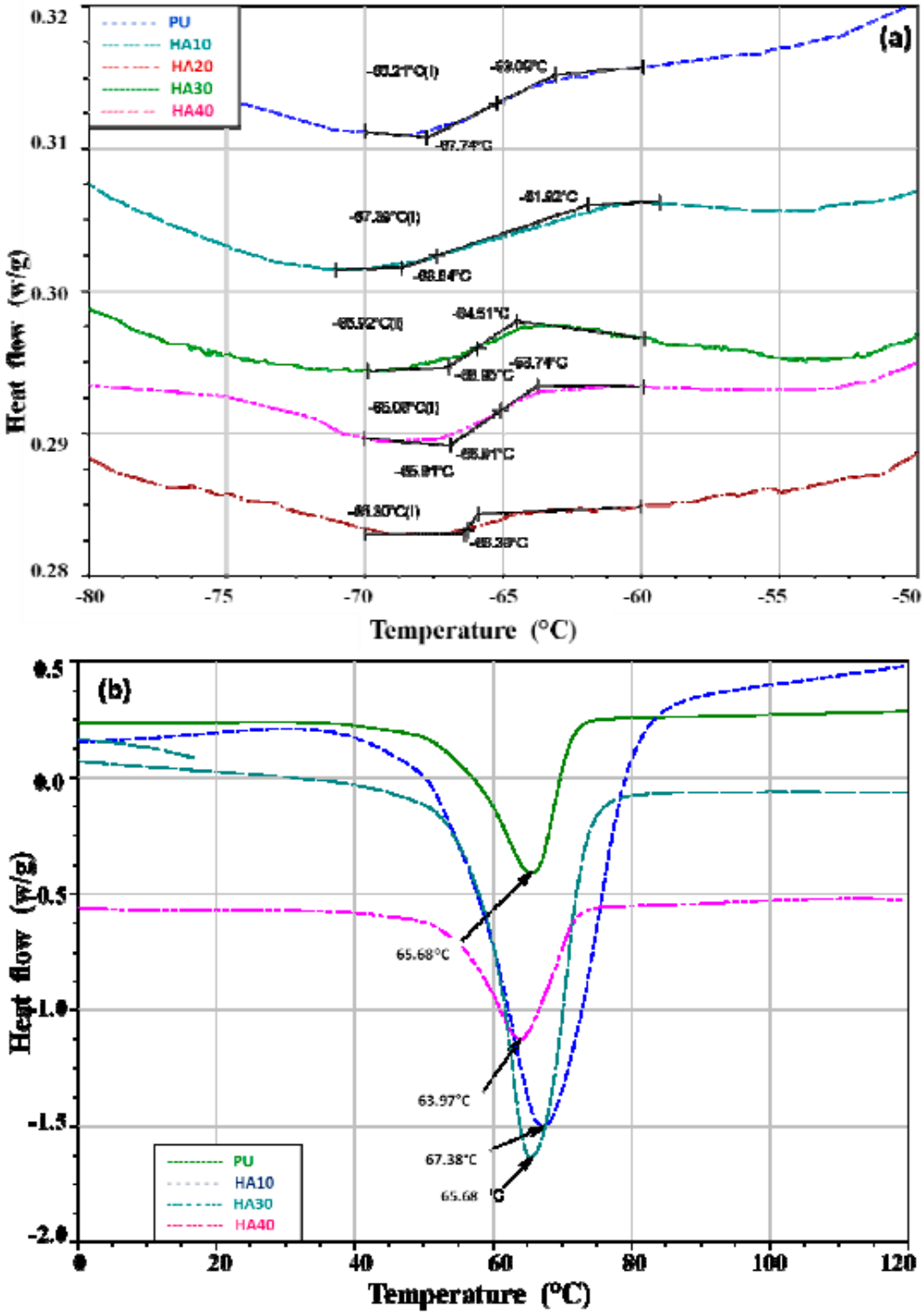

Figure 10. DSC scans of hybrids, (a) glass transition (tg) and (b) melting events (T_m).

DSC analysis was carried out in order to study the thermal transition of PU and PU/nHA hybrids which were subjected to identical thermal treatments before DSC analysis to keep thermal history identical. The hybrids showed thermal transition in the range of -67 to -61°C (glass transition, t_g) determined on the point of inflection of the DSC scans (Figure 10a), this temperature decreases with increasing soft segment molecular weight for PU containing HDI (Rogulska et al., 2006). The results of melting events (Figure 10b) determined from strong endothermic peak, this result is in good agreement with the DTA analyses. A significant difference in T_g was not observed for the materials, the particle size of nHA is very small and do not influence the thermal properties of the hybrids.

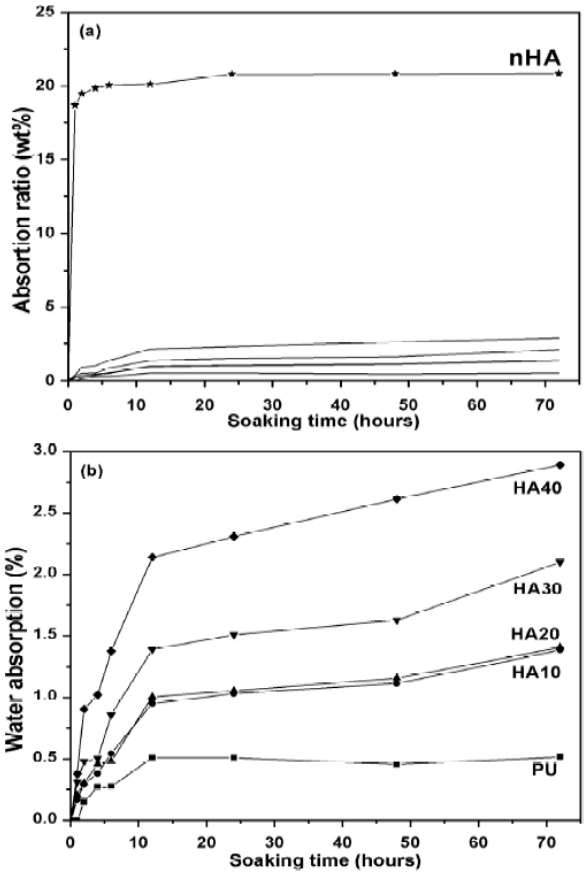

Figure 11. Water adsorption ratio curves of pure nHA (a) and PU/nHA hybrids (b).

It is very important to investigate the water absorption behavior of polymeric materials or composites of polymeric matrix due to the fact that both would have detrimental and beneficial effects on properties, for example decreasing the life of the composite by microcrack formation. Figures 11a and b show the water adsorption ratio curves of all materials synthesized from 0 to 40% nHA weight content, it can be observe that water absorption increase significantly with the incorporation of nHA in the polymer matrix (Figure 11b), that is the incorporation of nHA improve the hydrophilic ability of hybrids. It can to be attributed mainly to the internal interfaces formed between the polymer and the bioactive phases, major porosity (major surface area) for the incorporation the nHA and due to hydroxyl groups (OH^{-}).

Conclusions

Pure phase nHA which consist of nanocrystalline powders composed by submicrometric agglomerates, was prepared at low temperature through two different methods (hydrothermal crystallization and ultrasoundassisted coprecipitation) by the reaction of $Ca(NO_3)_2 \cdot 4H_2O$ and $(NH_4)_2HPO_4$ as raw materials. However ultrasound-assisted coprecipitation method reduced the time of synthesis of the nHA and leads nanometric characteristics (20 to 40 nm) and high surface area values (97.9 m^2g^{-1}), ideal to synthesized nanohybrid composites with better interaction filler-matrix. Biodegradable PU/nHA hybrids incorporating 0, 10, 20, 30, 40% weight of nHA were prepared by a two-step solution polymerization method and the nHA powders were homogeneously dispersed in PU matrix. The thermal stability of PU was increased by the incorporation of nHA in the hybrids and the absorption water increased with the

content of nHA. The results suggest that the nanohybrid could be adequate to apply in human body in the future.

Acknowledgments

The authors acknowledge the financial support from CONACYT from which A. B. Martinez-Valencia is fellow, as well as financial UMNSH-PTC-227 project. Furthermore, authors thank to D. Lardizabal G. and E. Torres M. for technical help and C. Ornelas for the use of probe aberration corrected high resolution electron microscope JEM-2200FS located in CIMAV Chihuahua, Mexico to the National Nanotechnology Laboratory (NANOTECH).

References

1.- Boccaccini AR, Gough JE (2007). Tissue engineering using ceramics and polymers. Woodhead-publishing, pp. 269-304.

2.- Dong ZH, Li Y, Zou Q (2009). Degradation and biocompatibility of porous nano-hydroxyapatite/polyurethane composite scaffold for bone tissue engineering. Appl. Surf. Sci., 255: 6087–6091.

3.- Dong ZH, Zhang L, Lia YB, Zhou G, Lee SW (2008). A guided bone regeneration membrane composed of hydroxyapatite and polyurethane. J. Ceram. Process. Res., 9: 478–481.

4.- Gedanken A (2004). Using sonochemistry for the fabrication of nanomaterials. Ultrason. Sonochem., 11: 47–55.

5.- Gorna K, Gogolewski S (2003). Preparation, degradation, and calcification of biodegradable polyurethane foams for bone graft substitutes. J. Biomed. Mater. Res., 67: 813–827.

6.- Griesser HJ (1991). Degradation of polyurethanes in biomedical applications: A review. Polym. Degrad. Stab., 33: 329–354.

7.- Guelcher SA (2008). Biodegradable polyurethanes: synthesis and applications in regenerative medicine. Tiss. Eng.: Part B., 14: 3–17.

8.- Kalita SJ, Bhardwaj A, Bhatt HA (2007). Nanocrystalline calcium phosphate ceramics in biomedical engineering. Mater. Sci. Eng., 27: 441–449.

9.- Leofantia G, Padovan M, Tozzola G, Venturelli B (1998). Surface area and pore texture of catalysts. Catal. Today, 41: 207–219.

10.- Lowell S, Shields JE, Thomas MA (2004). Characterization of porous solids and powders: Surface area, pore size and density. Particle Technology Series. Technical Report, Kluwer Academic Publishers.

11.- Nair LS, Laurencin CT (2007). Biodegradable polymers as biomaterials. Prog. Polym. Sci., 32: 762–798.

12.- Park JB, Bronzino JD (2003). Biomaterials, principles and applications. CRC Press, pp. 1-117.

13.- Ramakrishna S, Mayer J, Wintermatel E, Kam W, Leong W (2001). Biomedical applications of polymer-composites materials: A review. Compos. Sci. Technol., 61: 1189–1224.

14.- Rogers ME, Long TE (2003). Synthetic methods in step-growth polymers. John Wiley & Sons Inc., pp. 197-265.

15.- Rogulska M, Podkomcielny W, Kultys A, Pikus S, Posdzik E (2006). Studies on thermoplastic polyurethanes based on new

diphenylethane-derivative diols. I. Synthesis and characterization of nonsegmented polyurethanes from HDI and MDI. Eur. Polym. J., 42: 1786–1797.

16.- Santosa C, Clarke RL, Braden M, Guitian F, Davy KWM (2002). Water absorption characteristics of dental composites incorporating hydroxyapatite filler. Biomaterials, 23: 1897–1904.

17.- Silva CC, Pinheiro AG, Miranda MAR, Góes JC, Sombra ASB (2003). Structural properties of hydroxyapatite obtained by mechanosynthesis. Solid State Sci., 5: 553-558.

18.- Skarja GA, Woodhouse KA (2000). Structure-Property relationships of degradable polyurethane elastomers containing an amino acid-based chain extender. J. Appl. Polym. Sci., 75: 1522-1534.

19.- Suchanek W, Yoshimura M (1998). Processing and properties of hydroxyapatite-based biomaterials for use as hard tissue replacement implants. J. Mater. Res., 13: 94–117.

20.- Tkalcec E, Sauer M, Nonninger R, Schmidt H (2001). Sol-gel-derived hydroxyapatite powders and coatings. J. Mater. Sci., 36: 5253-5263.
Vermette P, Griesser HJ, Laroche G, Guidoin R (2001). Biomedical Applications of Polyurethanes. Landes Biosci., pp. 77-97.

21.- Wang M (2003). Developing bioactive composite materials for tissue replacement. Biomaterials, 24: 2133–2151.

22.- Zhao CX, Zhang WD (2008). Preparation of waterborne polyurethane nanocomposites: Polymerization from functionalized hydroxyapatite.

Eur. Polym. J., 44: 1988–1995.

23.- Zhao J, Guo LY, Yang XB, Weng J (2008). Preparation of bioactive porous ha/pcl composite scaffolds. Appl. Surf. Sci., 255: 2942–2946.

24.- Zhi-hua Z, Jian-ming R, Jian-peng Z, Zhong-cheng Z, Xiong-jun S (2007). Bioactivity of bioresorbable composite based on bioactive glass and poly-l-lactide. Trans. Nonferr. Met. Soc. China., 17: 394–4399.